

See discussions, stats, and author profiles for this publication at: <https://www.researchgate.net/publication/224183550>

Plasma-enabled growth of separated, vertically aligned copper-capped carbon nanocones on silicon

ARTICLE *in* APPLIED PHYSICS LETTERS · NOVEMBER 2010

Impact Factor: 3.3 · DOI: 10.1063/1.3502562 · Source: IEEE Xplore

CITATIONS

15

READS

26

4 AUTHORS, INCLUDING:



Shailesh Kumar

Queensland University of Technology

53 PUBLICATIONS 479 CITATIONS

SEE PROFILE



Kostya Ostrikov

The Commonwealth Scientific and Industri...

521 PUBLICATIONS 8,115 CITATIONS

SEE PROFILE

Plasma-enabled growth of separated, vertically aligned copper-capped carbon nanocones on silicon

S. Kumar,^{1,2} I. Levchenko,^{1,2} M. Keidar,³ and K. Ostrikov^{1,2,a)}

¹Plasma Nanoscience Centre Australia (PNCA), CSIRO Materials Science and Engineering, P.O. Box 218, Lindfield, New South Wales 2070, Australia

²Plasma Nanoscience, School of Physics, The University of Sydney, Sydney, New South Wales 2006, Australia

³Department of Mechanical and Aerospace Engineering, The George Washington University, Washington DC 20052, USA

(Received 10 September 2010; accepted 23 September 2010; published online 13 October 2010)

The formation of vertically aligned, clearly separated, copper-capped carbon nanocones with a length of up to 500 nm and base diameter of about 150 nm via three-stage process involving magnetron sputtering, N₂ plasma treatment, and CH₄+N₂ plasma growth is studied. The width of gaps between the nanocones can be controlled by the gas composition. The nanocone formation mechanism is explained in terms of strong passivation of carbon in narrow gaps, where the access of plasma ions is hindered and the formation of large C_nH_{2n+2} molecules is possible. This plasma-enabled approach can be used to fabricate nanoelectronic, nanofluidic, and optoelectronic components and devices. © 2010 American Institute of Physics. [doi:10.1063/1.3502562]

Owing to many unique mechanical, electrical, and thermal properties, vertically aligned nanostructures (nanocones, nanotubes, nanofibers, etc.) demonstrate an outstanding potential for the application as functional components of electron emission, nanoelectronic, nanomechanic, and other devices, environmental and biosensors, and scanning probe microscopes.^{1–3} In these applications, precise control of the structure, shape, and composition is required.^{4,5} Thus, the understanding of the processes and mechanisms of the effective growth control is crucial for numerous applications of nanostructures in modern devices.^{6,7}

Up to date, several advanced techniques have been developed for the production of vertically aligned nanostructures. Among others, low-temperature plasmas-based processes demonstrate improved controllability, with a strong effect of the plasma parameters on the nanostructure nucleation and growth.^{8,9} In many applications, the nanostructures should also be sharp, long, highly-conductive, and often capped with a highly-conductive metal (Au, Ag, and Cu). Carbon nanocones often satisfy these requirements. These nanocones are usually grown using ironlike metal catalyst nanoparticles which show a very high carbon solubility, such as Ni, Co, etc.¹⁰ These metals usually support the base-growth mode, i.e., the nanoparticles stay at the nanostructure base and do not form a cap. Besides, the carbon nanocones often coalesce during the growth (when the catalyst nanoparticles are close to each other), thus producing a larger structure with irregular shape. In this letter, we report on a plasma-enabled growth of clearly separated, vertically aligned, copper-capped carbon nanocones (CNCs) on a Si(100) surface. Scanning electron microscopy (SEM), TEM (transmission electron microscopy), energy-dispersive x-ray spectroscopy (EDS), and Raman techniques were used to reveal the shape, structure, and composition of the nanocones. A growth model was proposed to explain the clearly separated growth of nanostructures by strong passivation of

carbon in narrow gaps, where the access of the plasma ions is hindered and the formation of large hydrocarbon molecules is possible.

The capped carbon nanocones were grown in a low-frequency (13.56 MHz) inductively coupled plasma reactor [Fig. 1(a)] equipped with a quartz tube (10 cm dia.) and a dc (direct current) magnetron (not shown). The plasma was generated with the help of a helical rf coil around the tube. A dc bias was supplied to the substrate holder during the process. An SEM micrograph of typical carbon nanocones is shown in Fig. 1(b).

The process of nanocone fabrication involved the three main stages illustrated in Figs. 1(c)–1(f) and 2(a)–2(c). At the first stage [Fig. 1(c)], a continuous thin copper film (8 nm) was deposited on a Si (100) wafer by dc magnetron sputtering using a copper target [Figs. 1(d) and 2(a)]. Imme-

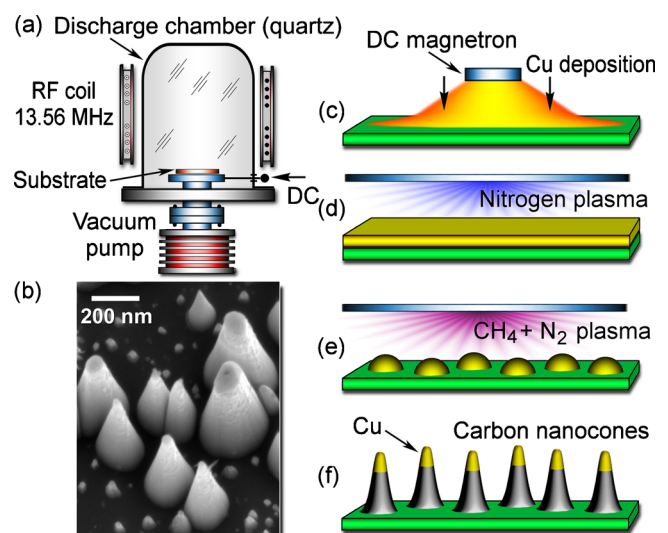


FIG. 1. (Color online) Scheme of the experimental setup (a), SEM micrograph of typical carbon nanocones (b). Panels (c)–(f) show the scheme of the process: magnetron deposition of a continuous Cu layer (c), treatment of the Cu layer in a nitrogen plasma to produce a Cu nanoparticle array (d), treatment of the Cu nanoparticle array in CH₄+N₂ plasmas (e), Cu-capped carbon nanocone array (f).

^{a)}Author to whom all correspondence should be addressed. Electronic mail: kostya.ostrikov@csiro.au.

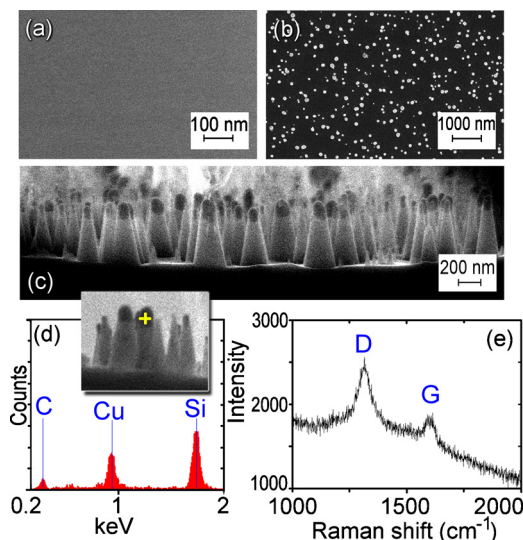


FIG. 2. (Color online) SEM images of the continuous film after magnetron sputtering deposition of copper onto a Si wafer (a); carbon nanocones grown on Cu nanoparticles (top view, low magnification) (b); carbon nanocones (side view) (c). Cu catalyst particles are clearly visible at the nanocone tops. EDS spectrum (d) taken from the nanocone top (SEM image on the inset, with the cross indicating the EDS spot) proves that the nanocone is Cu-capped. Raman characterization (e) shows clear D and G peaks evidencing that the nanocone base is made of pure carbon.

diately after that, the Cu film was processed in the nitrogen plasma for 5 min at the pressure of 4.0 Pa and the rf input power of 500 W. As a result, the copper film was fragmented into an array of copper nanoparticles with a mean size of 20–50 nm [Figs. 1(e) and 2(b)]. Next, the nanocone formation process was conducted in a $\text{CH}_4 + \text{N}_2$ ($\text{CH}_4 : \text{N}_2 = 1 : 1$) plasma at 15 Pa of the chamber pressure and 800 W of the rf input power for 15 min [Figs. 1(f) and 2(c)]. During the treatment in N_2 and $\text{CH}_4 + \text{N}_2$ plasmas, the substrate was biased with -25 V and -50 V, respectively. The surface temperature was maintained at 500°C in the N_2 plasma, and at 600°C in the $\text{CH}_4 + \text{N}_2$ plasma. No external substrate heating was used. No carbon nanocones appeared if a neutral $\text{CH}_4 + \text{N}_2$ gas mixture was used at the same pressure and background temperature.

A SEM image of the Cu film after magnetron sputtering deposition (stage 1 of the process) is shown in Fig. 2(a). From this figure one cannot trace any nanoparticles on the Si surface, and the copper film is continuous and homogenous. The SEM images of the carbon nanocones are shown in Figs. 2(b) and 2(c). The nanocones have a length of up to 500 nm and the base diameter of about 150 nm, with the tip diameters ranging from 10 to 50 nm. Apparently, the CNC size is determined by the size of Cu nanoparticle (Cu catalyst particles are clearly visible at the nanocones' tops). The EDS spectrum taken from the nanocone top (a cross on the SEM image shown in the inset) proves that the nanocone is Cu-capped [Fig. 2(d)]. Raman spectra have shown clear D and G peaks [Fig. 2(e)], thus evidencing that the nanocone base is made of pure carbon. The TEM image (Fig. 3) also reveals the graphitic structure of the nanocone's base. This image clearly shows the perfect "towerlike" shape with a massive, well-shaped copper top, with the top radius of approximately 10 nm. A copper cap length reaches 70–100 nm, and the cap base diameter reaches 50 nm.

Let us now examine in detail the growth of the nanocones in a close contact with each other. Some important

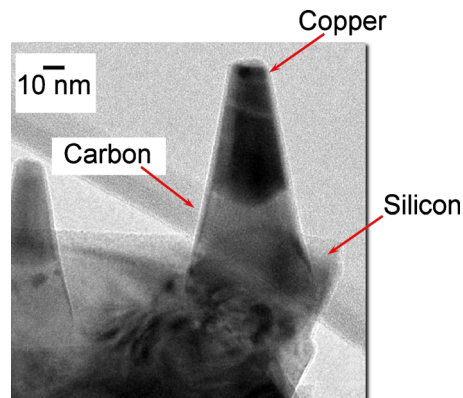


FIG. 3. (Color online) TEM image of a carbon nanocone with a copper catalyst particle on the top. The nanocone features a "towerlike" shape with a massive copper top.

observations can be made in Fig. 4, which depicts several groups ("nests") of closely located nanocones, alongside with "free-standing" nanostructures. It can be seen that the nanocones in these groups reshape to lean to each other but still remain closely separated. One can observe a very narrow gap between the nanocones, which is very clearly visible in the encircled fragments in Figs. 4(b) and 4(d). It is also seen that two individual (remote) nanocones at a relatively larger distance from each other (i.e., at the distance exceeding the base radius), grow symmetrically into two nanocones with round-shaped bases. The situation changes when a nanocone is located close to another nanocone (at the center-to-center

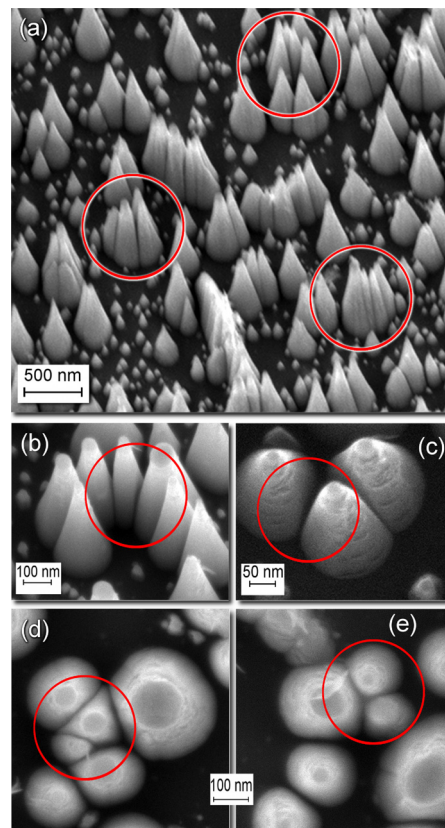


FIG. 4. (Color online) Tilted [(a)–(c)] and top-view [(d) and (e)] SEM images of the carbon nanocones. Groups (nests) of closely located nanocones are clearly visible. In the groups, nanocones reshape to lean to each other yet always remain clearly separated. Some representative nanocone groups are encircled.

distance of several tens of nanometer). In this case, the radial growth of the nanocone toward the neighboring nanocone slows down and then stops when the gap between the two nanostructures decreases to several nm. Interestingly, the radial growth in other directions still continues. As a result, the nanocone bases reshape to, e.g., triangle or other shape, depending on the specific number of the neighboring nanocones [it is clearly visible in Fig. 4(d)]. Finally, two closely located and reshaped nanocones continue growing still maintaining a tiny gap between them [in Fig. 4(d), the color contrast reveals a clearly visible gap between the nanocones].

Thus, we have fabricated vertically aligned carbon nanocones, always capped with copper nanoparticles. Moreover, these nanocones always remain clearly separated; we did not observe any coalescence and the formation of the merged nanostructure with an irregular shape. Instead, when the distance between the nanocones shrinks close to the threshold of several nanometers, the nanocones continue their reshaping *without a direct contact with each other and thus maintain the gap between them*. To obtain an insight into this phenomenon, we have conducted a series of additional experiments at the increased (up to 60%) N_2 concentration in the CH_4+N_2 gas mixture, and at the reduced surface temperature $T_s=500$ °C. When the process was conducted at a higher N_2 concentration, narrower gaps between the adjacent nanocones were formed, and a few nanocones coalesced together thus forming a large irregular nanostructure. The effect of the decreased surface temperature was not so pronounced; at $T_s=500$ °C, the nanocones still grew separately, but their shape slightly changed.

Let us now explain these observations, with the main attention paid to the formation of separated nanostructures. It is apparent that coalescence of several nanocones into a large structure is an energy minimization-driven thermokinetic process, due to a higher volume-to-surface ratio of the resulting nanostructure. Nevertheless, the coalescence appeared to be “forbidden” in our experiments. Thus, some additional process strongly changes the energy balance and ensures the stability of smaller nanostructures when the gap between the nanostructures becomes very narrow, i.e., when the surfaces of both closely located nanocones become involved in the process. Apparently, there is an effective mechanism of changing the energy balance of the nanostructures, namely, the formation of a layer making the nanocone stable at a small size, and preventing the otherwise unavoidable coalescence. Passivation of the nanostructure surface by hydrogen, which commonly leads to notable nanostructure reshaping in $Ar+H_2$ plasmas,¹¹ cannot prevent the coalescence by maintaining relatively large gaps of several nanometer. However, in the CH_4+N_2 plasma, the conditions for the synthesis of various hydrocarbons, are favorable due to the very high plasma density (up to 10^{18} – 10^{19} m⁻³), and the electron temperature of several eV.^{12–14} In this case, the surface-plasma sheath width is several tens of micrometer (for max. surface bias of 50 V). So, the sheath width significantly exceeds the typical nanocone length (0.5 μ m), and hence the influence of nanoscale-texturized electric field between the closely located nanocones cannot effectively draw the ions to the narrow gap. Thus, we propose the following growth mechanism of the clearly separated carbon nanocones. At the initial stage, when all nanocones are free-standing, an effective hydrogen termination of the side surfaces serves as a factor

promoting the nanostructure growth to form tall and sharp nanocones.¹⁵ Later, when the closely located nanocones form a small gap, and their temperature increases due to the strong ion flux-associated heating, the surface diffusion of large plasma-synthesized hydrocarbon molecules into the gap between the nanocones results in the formation of a hydrocarbonized layer on the nanocone walls. As a result, any penetration and incorporation of the carbon material into the nanocone from that side becomes impossible, and the radial growth toward the almost-contacting nanocone stops. Meanwhile, nitrogen ion bombardment (which can re-activate the surface by removing the passivating species) becomes ineffective due to very narrow gap between the nanocones. Indeed, when the process was conducted at the increased nitrogen concentration in the plasma, some nanocones coalesced. This probably happened due to the stronger nitrogen ion flux which reactivated some gaps for the growth.

These clearly separated copper-capped nanocones can be used in various applications. In particular, the narrow nanogaps between the nanocones grown on tailored catalyst nanopatterns can be promising for the fabrication of nanochannels in microfluidic devices such as filters incorporated into lab-on-a-chip platforms and for micro-organism and pathogen separation. Besides, these nanocones can be used as highly-conductive components with strong and conductive caps and a predetermined cross-section needed for nanomechanical, electrochemical, nanoelectronic, and energy conversion devices.

In summary, we have shown that the proposed plasma-enabled process is very effective for the fabrication of clearly separated, vertically aligned carbon nanocones capped with copper nanoparticles. The shape of the cross-section can be controlled by the catalyst pattern; the gaps between nanocones can be effectively controlled by the gas composition. Thus, components suitable for the nanoelectronic, nanomechanic, microfluidic, optoelectronic, sensing, energy conversion, and other applications can be fabricated.

¹U. Cvelbar, K. Ostrikov, A. Drenik, and M. Mozetic, *Appl. Phys. Lett.* **92**, 133505 (2008).

²K. Ostrikov, *Rev. Mod. Phys.* **77**, 489 (2005).

³M. K. Sunkara, S. Sharma, R. Miranda, G. Lian, and E. C. Dickey, *Appl. Phys. Lett.* **79**, 1546 (2001).

⁴I. Levchenko, K. Ostrikov, M. Keidar, and S. Xu, *Appl. Phys. Lett.* **89**, 033109 (2006); Z. L. Tsakadze, I. Levchenko, K. Ostrikov, and S. Xu, *Carbon* **45**, 2022 (2007).

⁵J. Shieh, C. H. Lin, and M. C. Yang, *J. Phys. D: Appl. Phys.* **40**, 2242 (2007).

⁶A. Shashurin and M. Keidar, *Carbon* **46**, 1826 (2008); I. Levchenko, K. Ostrikov, and D. Mariotti, *ibid.* **47**, 344 (2009).

⁷D. Mariotti, *Appl. Phys. Lett.* **92**, 151505 (2008).

⁸I. Levchenko and K. Ostrikov, *Appl. Phys. Lett.* **92**, 063108 (2008).

⁹M. Wolter, M. Stahl, and H. Kersten, *Plasma Processes Polym.* **6**, S626 (2009).

¹⁰A. V. Melechko, T. E. McKnight, M. A. Guillorn, V. I. Merkulov, B. Ilic, M. J. Doktycz, D. H. Lowndes, and M. L. Simpson, *Appl. Phys. Lett.* **82**, 976 (2003).

¹¹I. Levchenko, S. Y. Huang, K. Ostrikov, and S. Xu, *Nanotechnology* **21**, 025605 (2010).

¹²M. Mao and A. Bogaerts, *J. Phys. D: Appl. Phys.* **43**, 315203 (2010).

¹³I. Denysenko and K. Ostrikov, *Appl. Phys. Lett.* **90**, 251501 (2007).

¹⁴S. Xu, I. Levchenko, S. Y. Huang, and K. Ostrikov, *Appl. Phys. Lett.* **95**, 111505 (2009).

¹⁵I. Levchenko, O. Ostrikov, J. D. Long, and S. Xu, *Appl. Phys. Lett.* **91**, 113115 (2007).